JSHC
Japan Society of
Histochemistry and Cytochemistry
Established 1959

Acta Histochem. Cytochem. 51 (1): 1–8, 2018
doi: 10.1267/ahc.17030

Review

A Newly Defined Area of the Mouse Anterior Hypothalamus Involved in Septohypothalamic Circuit: Perifornical Area of the Anterior Hypothalamus, PeFAH

Noriko Horii-Hayashi and Mayumi Nishi

Department of Anatomy and Cell Biology, Nara Medical University, Kashihara, Nara 634–8521, Japan

Received October 10, 2017; accepted October 25, 2017; published online February 21, 2018

Although the hypothalamus is classified into more than 10 compartments, it still contains uncharacterized areas. In this study, we identified a new triangular-shaped area between the paraventricular hypothalamic nucleus (PVN) and the fornix area in the mouse anterior hypothalamus, which is enriched in chondroitin sulfate proteoglycans (CSPGs). We designated this region as the perifornical area of the anterior hypothalamus (PeFAH) based on its anatomical location. As evidenced by Nissl staining, the PeFAH was distinguishable as an area of relatively low density. Immunohistochemical and DNA microarray analyses indicated that PeFAH contains sparsely distributed calretinin-positive neurons and densely clustered enkephalin-positive neurons. Furthermore, the PeFAH was shown to have bidirectional neural connections with the lateral septum. Indeed, we confirmed enkephalinergic projections from PeFAH neurons to the lateral septum, and inversely, calbindin-positive lateral septum neurons as afferents to the PeFAH. Finally, c-Fos expression analysis revealed that the activity of certain PeFAH neuronal populations tended to be increased by psychological stressors, but not that of enkephalinergic neurons. We proposed PeFAH as a new region in the AH.

Key words: perifornical area, lateral septum, enkephalin, calretinin, perineuronal net

I. Introduction

Based on previous studies and brain atlases, the hypothalamus is subdivided into many nuclei and areas. However, there still remain uncharacterized hypothalamic regions. Recent studies suggested that the hypothalamic neurons involved in the regulation of metabolism, stress response, and reproduction remain plastic through adulthood [9, 10, 15, 17–19, 21]. The paraventricular nucleus of the hypothalamus (PVN) is one such region that remains plastic throughout life and controls stress responses by the hypothalamic-pituitary-adrenal axis. The number of synapses and the shape of glial cells in the PVN are dramatically altered in response to osmotic and psychological stressors [15, 17].

Neural plasticity is modulated not only by synaptic changes but also by structural alterations of the extracellular matrix (ECM). Perineuronal nets (PNNs) are specialized ECM structures that cover the somata and proximal dendrites of certain types of neurons with a lattice-like meshwork. The PNNs are composed of molecules such as chondroitin sulfate proteoglycans (CSPGs), hyaluronan, hyaluronan and proteoglycan link proteins (HAPLNs), and some glycoproteins [7, 8]. Ocular dominance plasticity is restored by destruction of PNNs in the adult visual cortex following injection of chondroitinase ABC (ChABC) [24]. The same treatment in the adult amygdala erases fear memories [13].

Many studies have focused on PNNs in the cerebral cortex and limbic system, where the majority of PNNs surround parvalbumin (PARV)-positive inhibitory neurons

Correspondence to: Mayumi Nishi, M.D., Ph.D., Department of Anatomy and Cell Biology, Faculty of Medicine, Nara Medical University, Kashihara, Nara 634–8521, Japan. E-mail: nmayumi@naramed-u.ac.jp

This paper was presented as Takamatsu Prize Lecture in 58th Annual Meeting of Japan Society of Histochemistry and Cytochemistry (Ehime 2017).

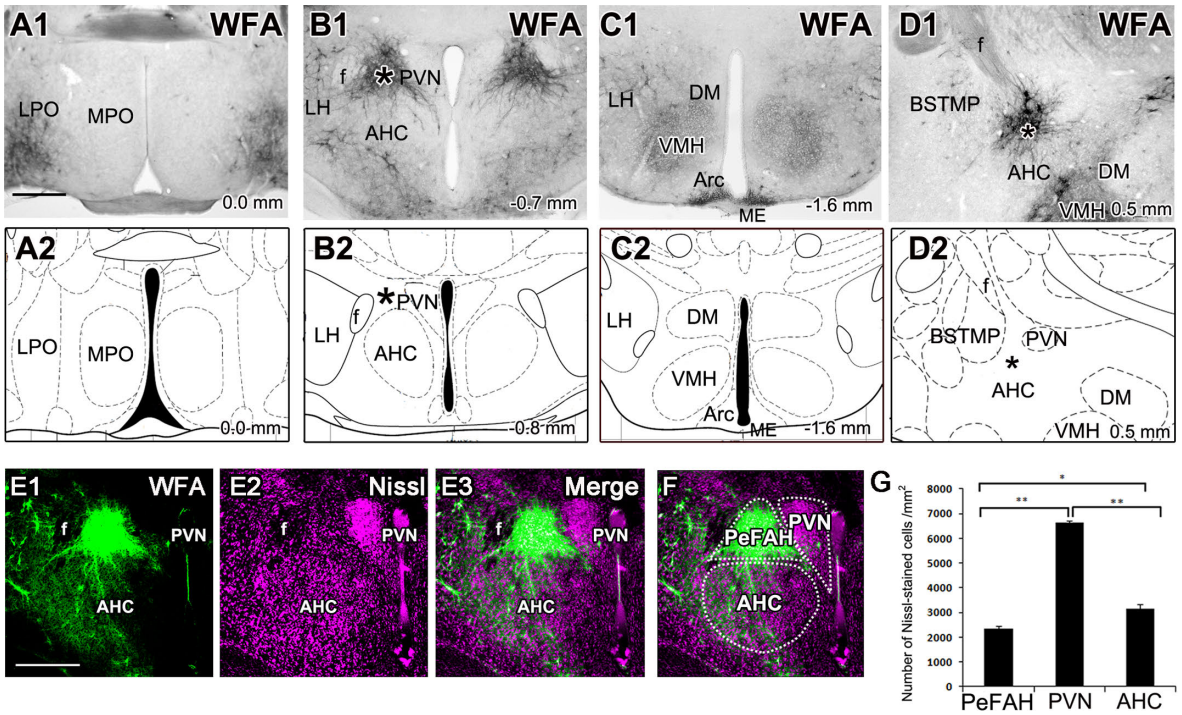

Fig. 1. The WFA labeling reveals a new hypothalamic region between the PVN and the fornix. (**A–D**) A series of WFA-labeled coronal (**A1–C1**) and sagittal (**D1**) sections and their approximate diagrams in the mouse brain atlas (**A2–D2**). Numerical values indicate the distance from bregma (**A–C**) or the midline (**D**). Note that the highly WFA-stained region in **B1** or **D1** (asterisks) is not designated in the coronal or sagittal atlas (**B2**, **D2**, asterisks). (**E, F**) Double labeling of WFA and Nissl indicates that the WFA-labeled region can be identified as a triangle-shaped region with a sparse distribution of Nissl-stained cells (**E**) and regional definitions of the PeFAH, PVN, and AHC (**F**). (**G**) Quantitative results of the density of Nissl-stained cells in the PeFAH, PVN, and AHC, demonstrating a lower density in the PeFAH than that in the PVN and AHC (mean ± standard error of the mean, one-way analysis of variance, Tukey's *post-hoc* test, * $P < 0.01$, ** $P < 0.0001$, n = 3). Bars = 500 μm (**A–D, E, F**). Arc, arcuate nucleus; AHC, central part of the anterior hypothalamic area; BSTMP, bed nucleus of the stria terminals, medial part; DM, dorsomedial hypothalamic nucleus; f, fornix; LH, lateral hypothalamic area; LPO, lateral preoptic area; ME, median eminence; MPO, medial preoptic nucleus; PeFAH, perifornical area of anterior hypothalamus; PVN, paraventricular nucleus; VMH, ventromedial hypothalamic nucleus; WFA, *Wisteria floribunda* agglutinin.

[2, 6, 14, 20, 23, 27]. However, only few studies have reported on the formation and function of PNNs in the hypothalamus. The lectin *Wisteria floribunda* agglutinin (WFA) binds to carbohydrate structures terminated by N-acetylgalactosamine and is often used for detecting chondroitin sulfate and PNN [3, 4, 27]. When we observed PNN formation in the mouse hypothalamus using WFA staining, we found a strongly labeled region surrounded by the fornix, PVN, and central division of the anterior hypothalamus (AHC). Since this region had not been described in the mouse brain atlas [11] or elsewhere, we named it "perifornical area of the anterior hypothalamus (PeFAH)" based on its anatomical location and its lower neuronal density evaluated by Nissl staining (Fig. 1E). The aim of this review was to characterize neuronal components, neuronal connections, and neuronal reactivity of the PeFAH. We first identified the PeFAH neuronal subtypes by histological and DNA microarray analyses. Second, we investigated the connections of this region by neuronal tract tracing. Third, to elucidate the reactivity of PeFAH neurons, we analyzed the pattern of c-Fos expression as an indicator of neuronal activity after exposure to psychological or homeostatic stressors.

II. A New Hypothalamic Area Enriched in CSPGs

The WFA labeling in the mouse hypothalamus resulted in a weak signal in the medial preoptic nucleus (Fig. 1A), PVN (Fig. 1B), and dorsomedial hypothalamic nucleus (Fig. 1C). In contrast, the signal was clearly detected in the lateral preoptic area (Fig. 1A), lateral hypothalamic area (Fig. 1B, C), ventral side of the central part of the anterior hypothalamic area (AHC) (Fig. 1B), and ventromedial hypothalamic nucleus (Fig. 1C). In the arcuate nucleus, only the ventral border neighboring the median eminence was densely labeled with WFA (Fig. 1C). Notably, a region surrounded by the fornix, PVN, and AHC was densely labeled with WFA (Fig. 1B), and was located at approximately 0.7 mm posterior from bregma. The region that we designated PeFAH was not described in the mouse brain atlas [11] (Fig. 1B2). We also confirmed the position of this region using sagittal sections, and observed a strongly WFA-labeled region caudal to the medial posterior part of the bed nucleus of the stria terminalis (Fig. 1D), which was situated at approximately 0.45 mm lateral from the midline. As in the coronal atlas, this WFA-labeled

region is not specifically designated in the sagittal atlas (Fig. 1D2). Double staining with Nissl and WFA showed that the boundary of the WFA-labeled triangular region could be distinguished by Nissl staining (Fig. 1E). Nissl-stained cells in the PeFAH, PVN, and AHC were quantitatively analyzed (Fig. 1G). The density of Nissl-stained cells in the PeFAH (2356 ± 107 cells/mm^2, n = 3) was significantly lower than that in the PVN (6644 ± 50 cells/mm^2, $P < 0.0001$, *post-hoc*) and AHC (3159 ± 188 cells/mm^2, $P < 0.01$, *post-hoc*; Fig. 1G). These results indicated that the PeFAH is a single compartmented area that could be distinguished from the PVN and AHC by WFA or Nissl staining.

The WFA signal in the PeFAH disappeared at the site of a ChABC injection (Fig. 2A), indicating that this signal was specifically derived from the chondroitin sulfate. Since a previous study demonstrated that WFA mainly recognizes a carbohydrate epitope on aggrecan, a major CSPG component of PNNs [12], we performed aggrecan staining with the anti-Cat-315 antibody. The Cat-315 immunoreactivity also exhibited the triangular shape of the region between the fornix and PVN (Fig. 2B). Double labeling of WFA and arginine vasopressin (AVP), a highly expressed neuropeptide in the PVN, revealed adjacent but hardly overlapped signals (Fig. 2C). Additionally, double labeling of WFA and NeuN or microtubule-associated protein 2 (MAP2) indicated that the WFA signal encompassed the somata of NeuN-labeled neurons (Fig. 2D) or MAP2-labeled dendrites (Fig. 2E). These results indicate that the PeFAH includes PNN-positive neurons. However, WFA staining in the PeFAH is subtly incompatible with the common morphological structures of PNNs showing a lattice-like meshwork [8]. Indeed, WFA reactivity was particularly thick around the somata, but was diffuse around the dendrites, and no clear lattice-like meshwork could be perceived. Thus, the ECM structures around PeFAH neurons seem not to be typical PNNs. Furthermore, unlike the lateral hypothalamic area and the cerebral cortex, the expression of HAPLN1, also known as cartilage link protein 1, which is an important molecular component of the highly specialized PNNs structures [5], was not detected in PeFAH.

Interestingly, each hypothalamic nucleus/area, including the PeFAH, shows a characteristic WFA staining pattern. For example, medial hypothalamic structures such as the medial preoptic area, PVN, and dorsomedial hypothalamic nucleus show lower WFA staining, while the lateral preoptic area and the lateral hypothalamic area include PNN-positive neurons. Thus, it is thought that each region has its own characteristic extracellular environment, which may lead to differences in neural plasticity and/or cationic conditions. According to the hypothesis that PNNs limit plasticity, the plasticity of PeFAH neurons may be highly restricted by perineuronal and perisynaptic sheaths enriched in CSPGs. However, since animals lacking HAPLN1 are known to exhibit persistent visual plasticity [5], further studies are required to assess the functions of CSPGs in the PeFAH, which we plan to carry out.

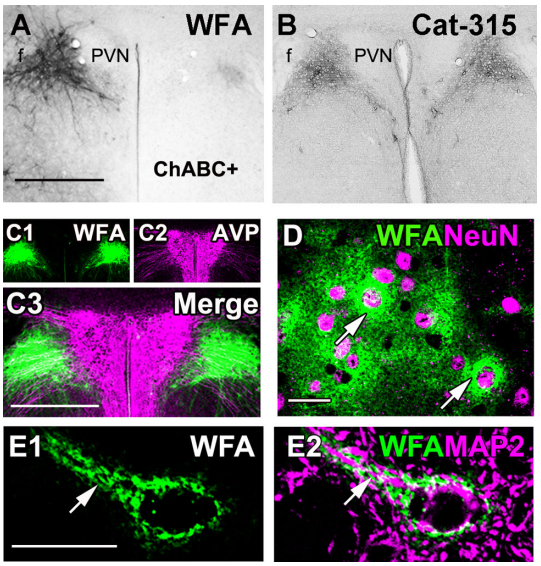

Fig. 2. The PNN-positive neurons in the PeFAH. (**A**) The left side of the image shows a WFA-stained PeFAH between the fornix and PVN, while unilateral injection of ChABC abolished the WFA signal in the injected side (the right side of the picture). (**B**) Immunohistochemical staining with anti-Cat-315 antibody indicating an aggrecan-immunoreactive region with a triangular shape between the fornix and PVN. (**C**) Double labeling of WFA and AVP shows an adjacent but non-overlapping distribution of the PeFAH and PVN. (**D**) Double labeling of WFA (green) and NeuN (magenta) reveals NeuN-labeled neurons surrounded by PNN (arrows). (**E**) Double labeling of WFA (green) and MAP2 (magenta) indicates a sheath of PNNs around a MAP2-labeled dendrite (arrows). Bars = 500 μm (**A, B, C**) and 50 μm (**D, E**). AVP, arginine vasopressin; ChABC, chondroitinase ABC; f, fornix; PeFAH, perifornical area of the anterior hypothalamus; PNN, perineuronal net; PVN, paraventricular nucleus; WFA, *Wisteria floribunda* agglutinin.

III. Characterization of PeFAH by Microarray and Histological Analyses

Microarray analysis was performed to screen for neurotransmitters, peptides, and neuronal marker proteins expressed in the PeFAH and PVN. Gene expression levels were analyzed based on the log2-transformed signal intensity of each gene. Genes for glutamatergic (*Slc1a1* and *Slc17a6*) and gamma-aminobutyric acid (GABA)-ergic (*Gad1*, *Gad2*, and *Slc6a1*) markers showed high expression in both the PeFAH and PVN. However, monoaminergic (*Slc6a2*, *Slc6a4*, and *Th*) and cholinergic (*Chat*) markers showed lower expression in the PeFAH, while *Th* expression in the PVN was moderate. Compared to the PeFAH, the PVN showed higher expression levels of *Avp*, *Crh*, *Oxt*, and *Sst*, which encode for AVP, corticotropin-releasing hormone (CRH), oxytocin (OXT), and somatostatin, respectively, and lower expression levels of *Penk*, which encodes for methionine-Enk (M-Enk) and leucine-Enk (L-Enk). Among genes for calcium-binding proteins, *Calb2* was prominently expressed in both regions.

The expression of the majority of the above-mentioned genes was investigated by immunohistochemistry, occasionally using colchicine-treated mice, in cases of detecting M-Enk, L-Enk, GABA, AVP, CRH, OXT, hypocretin, and vesicular glutamate transporter 2 (VGLUT2). Prominent somatic expression of M-Enk, L-Enk, calretinin (CALR, product of *Calb2*), and GABA were detected in the PeFAH (Fig. 3). However, substantial soma-like signals of the following neurotransmitters and calcium-binding proteins could not be observed in the PeFAH: AVP, CRH, OXT, somatostatin, hypocretin (product of *Hcrt*), PARV (product of *Pvalb*), calbindin (CALB, product of *Calb1*), choline acetyltransferase (product of *Chat*), and tyrosine hydroxylase (product of *Th*). Punctate signal of VGLUT2 (product of *Slc17a6*), probably derived from synaptic signal, was clearly detected in the PeFAH, while its soma-like signal was not detected even in colchicine-treated mice. Double labeling with WFA and M-Enk revealed a prominent cluster of Enk-positive neurons in the dorsal portion of the PeFAH in colchicine-treated mice (Fig. 3A). The same result was obtained when colabeling with L-Enk. Double labeling of WFA and CALR indicated many CALR-positive neurons dispersed in the PeFAH (Fig. 3B). Higher magnification views of double labeling of WFA with M-Enk or CALR revealed that some of the Enk- or CALR-positive neurons were surrounded by CSPGs (Fig. 3C, D). We also investigated GABA expression in Enk- and CALR-positive neurons in colchicine-treated mice. Although some GABA-positive somata were detected in the PeFAH, both M-Enk- and CALR-positive neurons were GABA-negative (Fig. 3E, F). These results indicated that at least three types of neurons exist in the PeFAH: Enk-positive/GABA-negative, CALR-positive/GABA-negative, and GABA-positive. Furthermore, we compared the expression pattern in two different mouse strains; in both BALB/c and ICR mice, a strongly WFA-labeled region was observed between the fornix and the PVN, which contained a cluster of L-Enk-positive neurons (Fig. 3G, H).

The immunohistochemical results were consistent with those of the DNA microarray analysis. Additional confirmation from *in situ* hybridization data from the Allen Brain Atlas indicated that *Calb2* (Exp No. 79556662) and *Penk* (Exp. No. 74881286) are highly expressed in the region presumed to be the PeFAH. A few *gad1*-positive cells were detected in the same region, whereas the signals for *Pvalb* (Exp. No. 868) and *Calb1* (Exp. No. 79556672) were hardly detected.

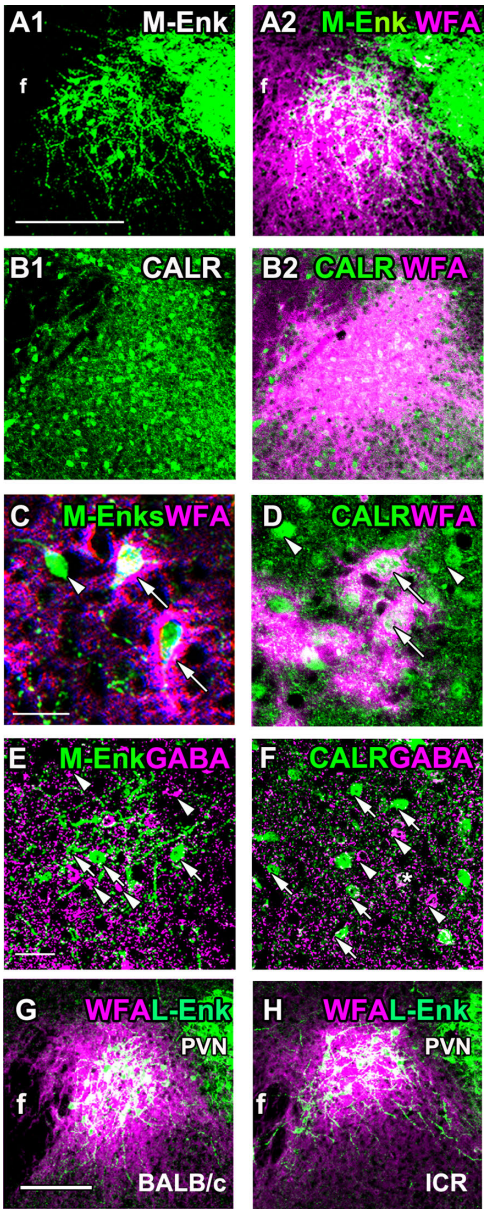

Fig. 3. Neuronal subtypes in the PeFAH. (**A–D**) Fluorescent images show double labeling of WFA (magenta) and M-Enk (green) or CALR (green) at lower (**A, B**) and higher (**C, D**) magnifications. The M-Enk-positive neurons (**A**) were identified as a cluster located dorsally in the PeFAH, while CALR-positive neurons (**B**) were spread out throughout the PeFAH. Some M-Enk- (**C**) or CALR-positive (**D**) neurons are surrounded by PNNs (arrows), and some are not (arrowheads). (**E, F**) Double labeling of GABA (magenta) with M-Enk (green) or CALR (green) showing that M-Enk- (**E**) or CALR-positive (**F**) neurons (arrows) are GABA-negative, and GABA-positive neurons (arrowheads) are M-Enk- or CALR-negative. (**G, H**) Labeling with WFA (magenta)/L-Enk (green) in colchicine-treated BALB/c (**G**) or ICR (**H**) mice. A cluster of L-Enk positive neurons is observed in a WFA-labeled region between the PVN and the fornix. Bars = 250 μm (**A, B, G**), 50 μm (**C, E**). AHC, central part of the anterior hypothalamic area; CALR, calretinin; f, fornix; GABA, gamma-aminobutyric acid; L-Enk, leucine-enkephalin; M-Enk, methionine-enkephalin; PVN, paraventricular nucleus; WFA, *Wisteria floribunda* agglutinin.

IV. Neural Networks of the PeFAH Neurons

Projections from the PeFAH were investigated with the anterograde tracer biotinylated dextran amine (BDA) (Fig. 4A). The micrograph of the injection site indicated the specific injection of BDA into the PeFAH (Fig. 4B). A massive ipsilateral projection to the lateral septum (LS) was observed, in which BDA-reactive fibers were detected

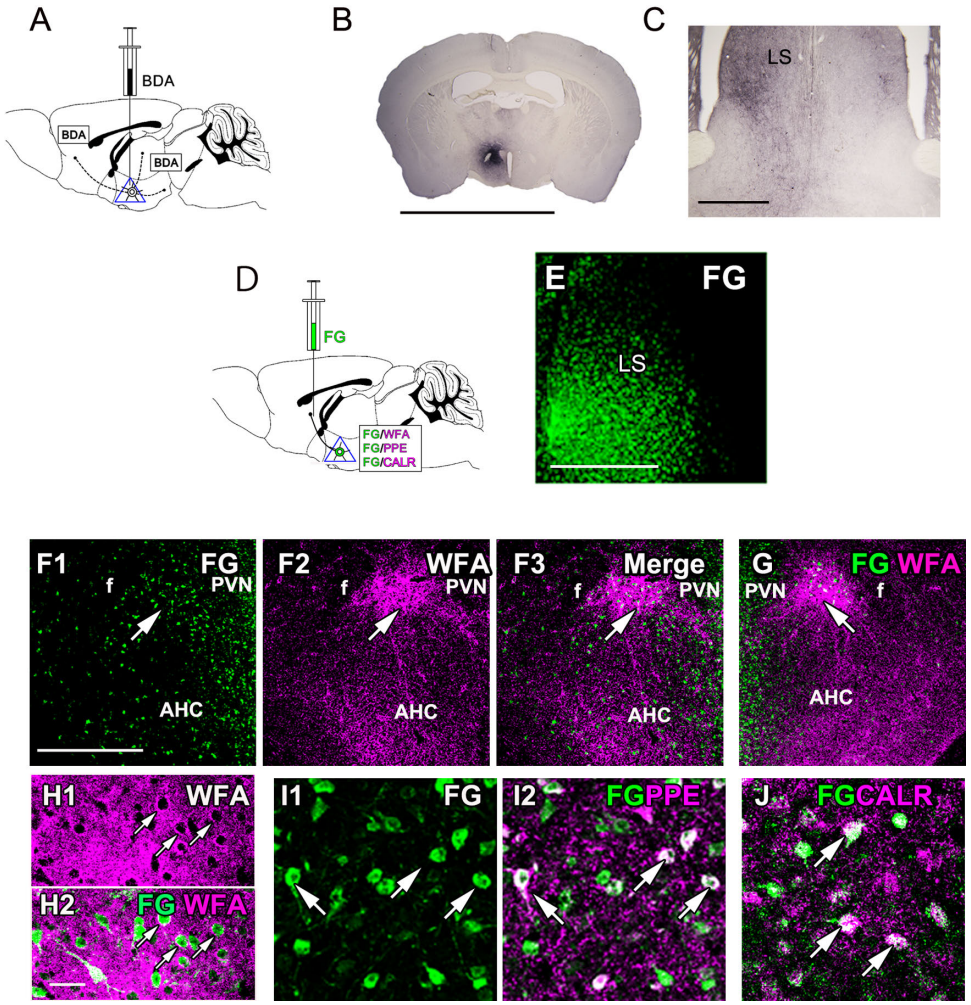

Fig. 4. Projections of PeFAH neurons. (**A**) A diagram illustrating the anterograde tracing with BDA in the PeFAH. (**B**) The BDA reaction at the injection site. (**C**) Many BDA-reactive fibers are observed ipsilaterally in the LS. (**D**) A diagram illustrating the retrograde tracing with FG applied to the LS neurons, which is followed by the detection of FG/WFA, FG/PPE, and FG/CALR in the PeFAH. (**E**) The FG signal at the injection site. (**F–H**) Double labeling of FG (green) and WFA (magenta) shows FG-labeled neurons in the PeFAH in both ipsilateral (**F**, arrows) and contralateral (**G**, arrow) sides. Higher magnifications reveal FG-labeled neurons surrounded by PNNs (**H**, arrows). (**I, J**) Double labeling of FG (green) and PPE (magenta) or CALR (magenta) demonstrating overlap of FG-labeled neurons with PPE-positive (**I**, arrows) or CALR-positive (**J**, arrows) neurons. Bars = 5 mm (**B**), 500 µm (**C, F, G**), 250 µm (**E**), and 50 µm (**H–J**). AHC, central part of the anterior hypothalamic area; BDA, biotinylated dextran amine; CALR, calretinin; f, fornix; FG, Fluoro-Gold; LS, lateral septum; PPE, preproenkephalin; PVN, paraventricular nucleus; WFA, *Wisteria floribunda* agglutinin.

extensively (Fig. 4C). A few BDA-reactive fibers were also detected in the contralateral side. Projection of PeFAH neurons to the LS was confirmed by retrograde tracing with Fluoro-Gold (FG) (Fig. 4D; injection site shown in Fig. 4E). Many FG-positive cells were observed on both sides of the PeFAH (Fig. 4F–H). Part of the FG-positive cells overlapped with preproenkephalin-positive and CALR-positive neurons (Fig. 4I, J), indicating that Enk- and CALR-positive PeFAH neurons project to the LS.

Retrograde tracing with cholera toxin B (CTb) was subsequently performed to identify afferents to the PeFAH (Fig. 5A, B). The CTb-positive cells were detected ipsilaterally over a wide extent of the LS (Fig. 5C). The majority of LS neurons are known to be GABAergic, and express both CALB and CALR [29]. Lower-magnification views revealed a shared distributed pattern between CTb-labeled LS neurons and CALB-positive neurons (Fig. 5D). The CTb-labeled neurons partly overlapped with CALB-positive neurons (Fig. 5E).

Although the medial hypothalamus and the LS have reciprocal neural connections, the relevant neuronal subtypes and anatomical details have not been fully elucidated. Our tracing studies revealed direct inputs from CALB-positive LS neurons to the PeFAH, which is the first evidence of projections from LS neurons to the hypothalamus. Since CALB-positive LS neurons are GABAergic [29], PeFAH neurons would presumably receive inhibitory regulation from LS. Interestingly, a previous study in rats demonstrated that Enk-positive fibers from the hypothalamus terminate on CALB-positive neurons in the LS [28].

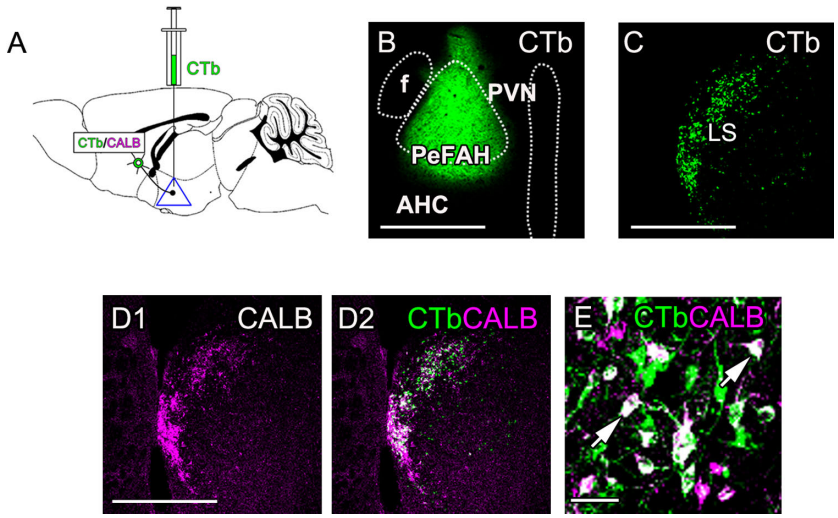

Fig. 5. Afferents of the PeFAH region. (**A**) A schematic diagram illustrating retrograde tracing with CTb in the PeFAH, which is followed by immunohistochemical detection of CALB in the LS. (**B**) A depiction of the injection site. (**C**) The CTb distribution in the LS. (**D, E**) Dual images of CTb (green) and CALB immunoreactivity (magenta) in the LS showing similar distributions of these two signals at lower magnification (**D**) and overlapping of CTb-labeled neurons with CALB-positive neurons at single-cell level (**E**, arrows). Bars = 500 μm (**B, C, D**) and 50 μm (**E**). AHC, central part of the anterior hypothalamic area; CALB, calbindin; CTb, cholera toxin B; f, fornix; LS, lateral septum; PeFAH, perifornical area of the anterior hypothalamus; PVN, paraventricular nucleus.

Therefore, several lines of evidence suggest the presence of a bidirectional connection between Enk-positive hypothalamic neurons and CALB-positive LS neurons.

V. Neuronal Responsiveness and Possible Functions

To clarify the reactivity of Enk-positive neurons in the PeFAH, we first examined the response of Enk-positive neurons to various stimuli by double-immunohistochemical staining with c-Fos and Enk. In non-stimulated controls, both group-housed and single-housed, the c-Fos expression was minimal in all regions analyzed. Following an open field trial (a novelty-stress model), c-Fos expression in Enk-positive neurons was not significantly increased relative to the control group. Furthermore, no c-Fos expression was observed in Enk-positive neurons. Similarly, aggression did not increase c-Fos expression in Enk-positive neurons. On the other hand, double labeling with WFA and GR showed prominent GR expression in the PeFAH.

Many studies have revealed c-Fos expression patterns in the PVN in response to various forms of stimulation. However, c-Fos activation in PVN neighboring regions is still poorly understood. Our results indicated no significant change in c-Fos expression in Enk-positive neurons in the PeFAH after restraint stress, open-field test, and aggression. In contrast, a certain neuronal population of PeFAH responded to these psychological stressors and showed an increase in c-Fos expression. Thus, these results suggest that, contradictory to many PVN neurons, c-Fos expression in Enk-positive PeFAH neurons does not respond to psychological stressors. A recent optogenetic study revealed that the pathway from LS neurons to the AH regulates the level of stress-induced anxiety [1]. According to this, the LS fibers labeled for optogenetic stimulation innervate the regions in and around the presumed PeFAH and the AHC. Thus, PeFAH neurons may be involved in emotional regulation under stressful conditions. However, functional roles for Enk-positive neurons in the AH have not been elucidated. The present data will enable future optogenetic and chemogenetic studies to clarify the functional roles of the neural circuits between the hypothalamus and the LS.

VI. Summary

In neuroanatomy, a “nucleus” is a cytoarchitectonic structure composed of a relatively compact cluster of neurons, while “area” is used to refer to a region composed of sparsely distributed neurons. According to this definition, the PeFAH is considered an “area.” A large number of studies using mice and rats reported the neuroanatomy of the PVN, while few studies addressed that of its neighboring regions, specifically in mice. In rats, the peri-PVN is an already characterized region located peripheral to the PVN [16]. However, although the histological location of the peri-PVN is very similar to that of the PeFAH, its neuronal components and projection targets are very distinct from those of the PeFAH, because the peri-PVN in rats is composed of abundant GABAergic neurons projecting to the PVN [16]. Previous studies in guinea pigs reported that a cluster of Enk-positive neurons projecting to the LS is located between the fornix and the PVN. This cluster is named the magnocellular dorsal nucleus (MDN) [25, 26]. Subsequently, a region homologous to the guinea pig

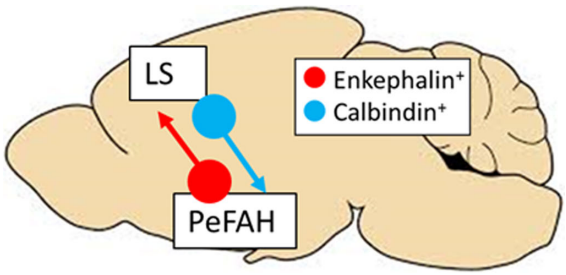

Fig. 6. Schema of the neural networks of the PeFAH. A schema showing the bidirectional connection between Enk-positive PeFAH neurons and CALB-positive LS neurons. LS, lateral septum; PeFAH, perifornical area of the anterior hypothalamus.

MDN, namely the perifornical nucleus (PeF), was identified in rats around the fornix at the PVN level. Considering the neuronal subtypes and projections, the cluster of Enk-positive neurons within the PeFAH would be comparable with the guinea pig MDN and the rat PeF. However, the PeFAH as a whole is larger than its Enk-positive region and is further characterized by a lower neuronal density and the presence of sparse CALR-positive neurons. Thus, it is reasonable to call the PeFAH a perifornical area [22].

In conclusion, we found and characterized a previously unidentified hypothalamic area, PeFAH, in the mouse brain between the fornix and the PVN. In addition to its WFA staining, the PeFAH is discriminable as an area of sparse Nissl staining and of a triangular shape as evidenced by immunohistochemical staining with the anti-Cat315 antibody. Moreover, histological and DNA microarray analyses elucidated that the PeFAH contains a cluster of GABA-negative neurons, namely Enk-positive and CALR-positive neurons. Neuronal tract tracing analyses indicated that the major projection target of PeFAH neurons is the LS and that they receive inputs from CALB-positive LS neurons, suggesting thus a bidirectional neural connection between the PeFAH and LS. Finally, c-Fos experiments suggested that Enk-positive neurons in the PeFAH do not exhibit reactivity to psychological stressors. Our ongoing optogenetic and chemogenetic studies will clarify the function of the neural circuits between the PeFAH and the LS, suggesting a new concept of septohypothalamic pathway (Fig. 6).

VII. Conflicts of Interest

The authors declare that there are no conflicts of interest.

VIII. Acknowledgments

This study was supported in part by a KAKENHI Grant-in-Aid for Scientific Research (15H04671) (MN) and (17K07080) (NH) and a KAKENHI Grant-in-Aid for Scientific Research on Innovative Areas “Willdynamics” (17H06060) (MN).

IX. References

1. Anthony, T. E., Dee, N., Bernard, A., Lerchner, W., Heintz, N. and Anderson, D. J. (2014) Control of stress-induced persistent anxiety by an extra-amygdala septohypothalamic circuit. *Cell* 156; 522–536.
2. Azuma, M., Tofrizal, A., Maliza, R., Batchuluun, K., Ramadhani, D., Syaidah, R., Tsukada, T., Fujiwara, K., Kikuchi, M., Horiguchi, K. and Yashiro, T. (2015) Maintenance of the extracellular matrix in rat anterior pituitary gland: identification of cells expressing tissue inhibitors of metalloproteinases. *Acta Histochem. Cytochem.* 48; 185–192.
3. Brauer, K., Hartig, W., Bigl, V. and Bruckner, G. (1993) Distribution of parvalbumin-containing neurons and lectin-binding perineuronal nets in the rat basal forebrain. *Brain Res.* 631; 167–170.
4. Bruckner, G., Seeger, G., Brauer, K., Hartig, W., Kacza, J. and Bigl, V. (1994) Cortical areas are revealed by distribution patterns of proteoglycan components and parvalbumin in the Mongolian gerbil and rat. *Brain Res.* 658; 67–86.
5. Carulli, D., Pizzorusso, T., Kwok, J. C., Putignano, E., Poli, A., Forostyak, S., Andrews, M. R., Deepa, S. S., Glant, T. T. and Fawcett, J. W. (2010) Animals lacking link protein have attenuated perineuronal nets and persistent plasticity. *Brain* 133; 2331–2347.
6. Celio, M. R. (1993) Perineuronal nets of extracellular matrix around parvalbumin-containing neurons of the hippocampus. *Hippocampus* 3; 55–60.
7. Celio, M. R. and Blumcke, I. (1994) Perineuronal nets—a specialized form of extracellular matrix in the adult nervous system. *Brain Res. Brain Res. Rev.* 19; 128–145.
8. Celio, M. R., Spreafico, R., De Biasi, S. and Vitellaro-Zuccarello, L. (1998) Perineuronal nets: past and present. *Trends Neurosci.* 21; 510–515.
9. Dietrich, M. O. and Horvath, T. L. (2013) Hypothalamic control of energy balance: insights into the role of synaptic plasticity. *Trends Neurosci.* 36; 65–73.
10. Flak, J. N., Ostrander, M. M., Tasker, J. G. and Herman, J. P. (2009) Chronic stress-induced neurotransmitter plasticity in the PVN. *J. Comp. Neurol.* 517; 156–165.
11. Franklin, K. B. J. and Paxinos, G. (2007) The Mouse Brain in Stereotaxic Coordinates, third ed., Academic Press, U.S.A.
12. Giamanco, K. A., Morawski, M. and Matthews, R. T. (2010) Perineuronal net formation and structure in aggrecan knockout mice. *Neuroscience* 170; 1314–1327.
13. Gogolla, N., Caroni, P., Luthi, A. and Herry, C. (2009) Perineuronal nets protect fear memories from erasure. *Science* 325; 1258–1261.
14. Hartig, W., Brauer, K. and Bruckner, G. (1992) Wisteria floribunda agglutinin-labelled nets surround parvalbumin-containing neurons. *Neuroreport* 3; 869–872.
15. Hatton, G. I. (1997) Function-related plasticity in hypothalamus. *Annu. Rev. Neurosci.* 20; 375–397.
16. Herman, J. P., Cullinan, W. E., Ziegler, D. R. and Tasker, J. G. (2002) Role of the paraventricular nucleus microenvironment in stress integration. *Eur. J. Neurosci.* 16; 381–385.
17. Herman, J. P., Flak, J. and Jankord, R. (2008) Chronic stress plasticity in the hypothalamic paraventricular nucleus. *Prog. Brain Res.* 170; 353–364.
18. Horvath, T. L. (2006) Synaptic plasticity in energy balance regulation. *Obesity (Silver Spring)* 14 Suppl 5; 228s–233s.
19. Keyser-Marcus, L., Stafisso-Sandoz, G., Gerecke, K., Jasnow, A., Nightingale, L., Lambert, K. G., Gatewood, J. and Kinsley, C. H. (2001) Alterations of medial preoptic area neurons following pregnancy and pregnancy-like steroidal treatment in

the rat. *Brain Res. Bull.* 55; 737–745.
20. Nakamura, M., Nakano, K., Morita, S., Nakashima, T., Oohira, A. and Miyata, S. (2009) Expression of chondroitin sulfate proteoglycans in barrel field of mouse and rat somatosensory cortex. *Brain Res.* 1252; 117–129.
21. Nishi, M. (2011) Dynamics of corticosteroid receptors: lessons from live cell imaging. *Acta Histochem. Cytochem.* 44; 1–7.
22. Onteniente, B., Menetrey, D., Arai, R. and Calas, A. (1989) Origin of the met-enkephalinergic innervation of the lateral septum in the rat. *Cell Tissue Res.* 256; 585–592.
23. Pantazopoulos, H., Lange, N., Hassinger, L. and Berretta, S. (2006) Subpopulations of neurons expressing parvalbumin in the human amygdala. *J. Comp. Neurol.* 496; 706–722.
24. Pizzorusso, T., Medini, P., Berardi, N., Chierzi, S., Fawcett, J. W. and Maffei, L. (2002) Reactivation of ocular dominance plasticity in the adult visual cortex. *Science* 298; 1248–1251.
25. Poulain, P. (1983) Hypothalamic projection to the lateral septum in the guinea pig an HRP study. *Brain Res. Bull.* 10; 309–313.
26. Poulain, P. (1986) Properties of antidromically identified neurons in the enkephalinergic magnocellular dorsal nucleus of the guinea pig hypothalamus. *Brain Res.* 362; 74–82.
27. Seeger, G., Luth, H. J., Winkelmann, E. and Brauer, K. (1996) Distribution patterns of Wisteria floribunda agglutinin binding sites and parvalbumin-immunoreactive neurons in the human visual cortex: a double-labelling study. *J. Hirnforsch.* 37; 351–366.
28. Szeidemann, Z., Shanabrough, M. and Leranth, C. (1995) Hypothalamic Leu-enkephalin-immunoreactive fibers terminate on calbindin-containing somatospiny cells in the lateral septal area of the rat. *J. Comp. Neurol.* 358; 573–583.
29. Zhao, C., Eisinger, B. and Gammie, S. C. (2013) Characterization of GABAergic neurons in the mouse lateral septum: a double fluorescence in situ hybridization and immunohistochemical study using tyramide signal amplification. *PloS One* 8; e73750.